

## New Test of the Friedmann-Lemaître-Robertson-Walker Metric Using the Distance Sum Rule

Syksy Räsänen

*Department of Physics, and Helsinki Institute of Physics, University of Helsinki,  
P.O. Box 64, FIN-00014 University of Helsinki, Finland*

Krzysztof Bolejko

*Sydney Institute for Astronomy, School of Physics, A28,  
The University of Sydney, Sydney, NSW 2006, Australia*

Alexis Finoguenov

*Department of Physics, University of Helsinki, P.O. Box 64, FIN-00014 University of Helsinki, Finland  
(Received 30 December 2014; revised manuscript received 2 July 2015; published 1 September 2015)*

We present a new test of the validity of the Friedmann-Lemaître-Robertson-Walker (FLRW) metric, based on comparing the distance from redshift 0 to  $z_1$  and from  $z_1$  to  $z_2$  to the distance from 0 to  $z_2$ . If the Universe is described by the FLRW metric, the comparison provides a model-independent measurement of spatial curvature. The test relies on geometrical optics, it is independent of the matter content of the Universe and the applicability of the Einstein equation on cosmological scales. We apply the test to observations, using the Union2.1 compilation of supernova distances and Sloan Lens ACS Survey galaxy strong lensing data. The FLRW metric is consistent with the data, and the spatial curvature parameter is constrained to be  $-1.22 < \Omega_{K0} < 0.63$ , or  $-0.08 < \Omega_{K0} < 0.97$  with a prior from the cosmic microwave background and the local Hubble constant, though modeling of the lenses is a source of significant systematic uncertainty.

DOI: [10.1103/PhysRevLett.115.101301](https://doi.org/10.1103/PhysRevLett.115.101301)

PACS numbers: 98.80.Es, 98.62.Py, 98.62.Sb, 98.80.Jk

*Introduction.—Testing the FLRW metric:* In addition to providing tight constraints on cosmological parameters in specific models, the increasing precision and breadth of cosmological observations makes it possible to test assumptions behind entire classes of models. A particularly important assumption is that the Universe is, on average, described by the exactly homogeneous and isotropic Friedmann-Lemaître-Robertson-Walker (FLRW) metric. More precisely, we consider the assumption that light propagation over long distances is described by the FLRW metric. This can be tested by consistency conditions between different observables derived from geometrical optics. Such tests are independent of the matter content of the Universe and its relation to spacetime geometry (usually given by the Einstein equation). It has been proposed that the observed late-time accelerated expansion could be related to the failure of the FLRW approximation. Possibilities include extra dimensions [1], violation of statistical homogeneity and isotropy [2], and the effect of deviation from exact homogeneity and isotropy on the average expansion rate, i.e., backreaction [3,4].

Testing the FLRW metric by comparing observations of the expansion rate and distance was proposed in [5] and implemented in [6–8]. A similar test using parallax distance and angular diameter distance was put forth in [9]. We propose a third consistency test, based on the sum rule of distances along null geodesics of the FLRW metric, and apply it to real data. If the sum rule is violated, the

FLRW metric is ruled out. If the data are consistent with the sum rule, the test provides a model-independent measurement of the spatial curvature of the Universe, like the tests proposed in [5,9].

*FLRW consistency condition.—Distances:* If space is exactly homogeneous and isotropic, spacetime is described by the FLRW metric

$$ds^2 = -dt^2 + \frac{a(t)^2}{1 - Kr^2} dr^2 + a(t)^2 r^2 d\Omega^2, \quad (1)$$

where  $K$  is a constant related to the spatial curvature; the Ricci scalar of the hypersurface of constant proper time is  $6K/a(t)^2$ . [When  $K > 0$ , the metric (1) covers only half of the spacetime.] The Hubble parameter is  $H \equiv \dot{a}/a$ , and its present value is denoted by  $H_0$ . Let  $D_A(z_l, z_s)$  be the angular diameter distance of a source at redshift  $z_s$  (emission time  $t_s$ ) as seen at redshift  $z_l$  (observation time  $t_l > t_s$ ). From (1), we find that the dimensionless distance  $d(z_l, z_s) \equiv (1 + z_s)H_0 D_A(z_l, z_s)$  is

$$d(z_l, z_s) = \frac{1}{\sqrt{-k}} \sinh \left( \sqrt{-k} \int_{t_s(z_s)}^{t_l(z_l)} \frac{H_0 dt}{a(t)} \right), \quad (2)$$

where  $k \equiv K/H_0^2$ . We denote  $d(z) \equiv d(0, z)$ .

*Distance sum rule:* Using (2),  $d_{ls} \equiv d(z_l, z_s)$  can be written in terms of  $d_l \equiv d(z_l)$  and  $d_s \equiv d(z_s)$  as

$$d_{ls} = \epsilon_1 d_s \sqrt{1 - kd_l^2} - \epsilon_2 d_l \sqrt{1 - kd_s^2}, \quad (3)$$

where  $\epsilon_i = \pm 1$ . For  $k \leq 0$ ,  $\epsilon_i = 1$ . For  $k > 0$ , the signs depend on which halves of the three-dimensional hypersphere the source and the lens are located and in which direction the light propagates. If there is a one-to-one correspondence between  $t$  and  $z$  and  $d'(z) > 0$ , then  $\epsilon_i = 1$ . We assume that this is the case, so we have

$$\frac{d_{ls}}{d_s} = \sqrt{1 - kd_l^2} - \frac{d_l}{d_s} \sqrt{1 - kd_s^2}. \quad (4)$$

The relation (3) [or (4)] is a sum rule for distances in the FLRW universe. [The case (4) is given in, e.g., [10], p. 336.] In the spatially flat case, the distances are simply added together, whereas for nonzero spatial curvature, the relation is more involved. Using (4) in the case  $|k| \ll 1$  to obtain a model-independent estimate of the spatial curvature was proposed in [11].

*The consistency condition:* The sum rule (3) has been derived from the FLRW metric. We get a consistency condition by solving for  $k$  to obtain (for all  $\epsilon_i$ )

$$k_S = -\frac{d_l^4 + d_s^4 + d_{ls}^4 - 2d_l^2 d_s^2 - 2d_l^2 d_{ls}^2 - 2d_s^2 d_{ls}^2}{4d_l^2 d_s^2 d_{ls}^2}, \quad (5)$$

where the subscript  $S$  indicates that  $k$  has been solved from the sum rule for distances. We now drop the assumption that the Universe is described by the FLRW metric and take (5) as the definition of a function  $k_S(z_l, z_s)$  in any spacetime (neglecting angular dependence). If the Universe is described by the FLRW metric,  $k$  is constant and equal to  $-\Omega_{K0}$ , the present value of the spatial curvature density parameter. If it is observationally found that  $k_S$  is different for any two pairs  $(z_l, z_s)$ , then light propagation on large scales is not described by the FLRW metric. The converse is not true: if  $k_S$  is constant, this does not imply that the metric is FLRW.

The consistency condition (5) provides a powerful test. In principle, the FLRW metric can be falsified by measuring the three quantities  $(d_l, d_s, d_{ls})$  for two different values of  $(z_l, z_s)$ . The test is very general, because it assumes only geometrical optics and that light propagation can be described with the FLRW metric. Unlike the condition between distance and expansion [5], the consistency condition (5) does not involve derivatives of the distance. Unlike the condition between angular diameter and parallax distances [9], there are already measurements of the distances involved,  $d$  and  $d_{ls}$ , on cosmological scales.

*Determining  $d$  and  $d_{ls}$ .*—*The distance  $d$ :* The Union2.1 compilation [12] provides luminosity distances  $D_L$  to 580 supernovae (SNe), with arbitrary overall normalization. The highest redshift in the compilation is 1.4. Normalizing by  $H_0$ , we obtain  $d_L \equiv H_0 D_L = (1+z)d$ , where the last relation holds in any spacetime [13]. Our test involves only ratios of distances, so it does not depend on the value of  $H_0$ .

In the Union2.1 analysis, the parameters that describe SN light curves are fitted at the same time as the cosmological parameters, and it is assumed that the Universe is described by the spatially flat FLRW model with dust and vacuum energy, so the resulting distances are model dependent [14]. There are also significant differences between light curve fitters [15]. However, such effects are likely subdominant to the uncertainties in the modeling of the strong lensing systems that we use to determine  $d_{ls}$ . We, therefore, simply use the distances to SNe given in [12], with the reported statistical and systematic errors.

*The distance  $d_{ls}$ :* Angular separation between strongly lensed images of the same source depends on  $d_{ls}/d_s$  and the structure of the lens. We assume that general relativity holds on the scale of the lensing system. If the lens can be approximated as a singular isothermal ellipsoid (SIE), we have [16]

$$\frac{d_{ls}}{d_s} = \frac{\theta_E}{4\pi f^2 \sigma^2}, \quad (6)$$

where  $\theta_E$  is the Einstein radius (in radians),  $\sigma$  is the velocity dispersion of the lens and  $f$  is a phenomenological coefficient that parametrizes uncertainty due to difference between the velocity dispersion of the observed stars and the underlying dark matter, and other systematic effects. Observations suggest the range  $0.8 < f^2 < 1.2$  [17,18].

We consider two different treatments of (6), which we call models Ia and Ib. In model Ia, we take  $f = 1$ . In model Ib, we model  $f$  by assigning an extra Gaussian error of 20% on  $d_{ls}/d_s$ . Leaving  $f$  as a free parameter would significantly degrade the constraints owing to a degeneracy between  $f$  and  $k$  for  $-k \gg 1$ , due to limited redshift coverage and the small number of lensing data points.

We also consider a more complicated treatment of the lens, introduced in [19], where (6) is replaced by  $d_{ls}/d_s = N(\alpha, \beta, \delta)(\theta_E^{\alpha-1}/4\pi\sigma^2)$ , with  $\alpha, \beta$ , and  $\delta$  being the slope of the density, anisotropy of the velocity dispersion, and the luminosity, respectively. We call this model II. Following [19], we treat  $\alpha$  and  $\beta$  as universal parameters with a Gaussian distribution with fixed mean and variance. For  $\delta$ , we use values reported for each individual lens. These depend on the aperture. We treat this variation as a lens-specific error on  $\delta$ , assumed to be Gaussian, with the  $1\sigma$  range given by the difference between the maximum and minimum values. The average mean value is  $\delta = 2.39$  and the average  $1\sigma$  error is 0.05. The values given in [19] are not centered around the SIE model, due to nonzero mean anisotropy in the velocity dispersion and the different slopes of the density and luminosity. For the mean values of  $\alpha$  and  $\beta$  and the value  $\delta = 2.4$  used in [19],  $d_{ls}/d_s$  is 12% lower than in the SIE case (6). In our best fits, the mean value of  $d_{ls}/d_s$  in model II is 8% lower than in model Ia, and 9% lower than in model Ib.

*Lensing data:* We select strong lensing systems for which there is a well-measured value for  $z_l, z_s, \theta_E$ , and  $\sigma$ . We require the lens to be either an elliptical or a lenticular galaxy, so that it can be modeled as a SIE. We also require that there is either an Einstein ring or arcs, not just multiple

images, because without individual spectra, we cannot be sure that separated images are from the same source. These criteria leave us with 30 lenses, listed in table II [20]. We have checked that the lenses are isolated from other galaxies and clusters. The data is mostly from the Sloan Lens ACS Survey [21], with additional data from the SIMBAD database [22] and [23]. The maximum source redshift is  $z_s = 0.98$ , well below the maximum redshift of 1.4 of the Union2.1 SN compilation. Following [21], we assign an error of 2% on  $\theta_E$  and a minimum error of 5% on  $\sigma$ .

*Data fit and results.—Fitting function:* In principle, the function  $k_S(z_l, z_s)$  defined in (5) can be reconstructed from observations, and if it is not constant, the FLRW metric is ruled out. Such a procedure has been applied to  $k$  defined with the expansion rate and distance [5] in [6,8]. However, (5) gives a biased estimate of  $k$ . If we insert values of  $d_l$ ,  $d_s$ , and  $d_{ls}$  with errors into (5), it will not be centred on the real value of  $k$ . In any case, given the small number of  $d_{ls}/d_s$  data points, we do not try to find  $k$  as a function of redshifts. Instead, we fit a constant  $k$  to the data and consider the goodness of fit. Large values of  $\chi^2/\text{d.o.f.}$  would be evidence against the FLRW model, or for unaccounted errors. If the FLRW hypothesis is not rejected, the  $\chi^2$  values give the probability distribution of  $k$ .

We obtain  $d(z)$  and  $k$  model independently by fitting to the SN and lensing data simultaneously. As the fitting function for  $d(z)$ , we have compared polynomials of different order, as well as splines, rational functions, and Bézier curves by fitting to mock data sets of FLRW models with zero, positive or negative spatial curvature, as well as the real data. We find that, with current data, it doesn't make much difference which function we use, as long as it is more flexible than a second order polynomial. Note that, in contrast to attempts to reconstruct the deceleration parameter or the equation of state [24], we do not need derivatives of  $d$ . We present the results for a fourth order polynomial. Because  $d(0) = 0$ ,  $d'(0) = 1$ , it has three parameters. Our fitting model, thus, consists of a fourth order polynomial for  $d(z)$ , and  $d_{ls}/d_s$  given by (4) with a constant  $k$ , with four parameters in total.

*Upper limit on  $k$  from CMB and  $H_0$ :* On a hypersphere, the comoving angular diameter distance is bounded from above by  $1/\sqrt{K}$ , so  $k \leq 1/d(z)^2$  for all  $z$ , and this applies our  $k$  defined by the sum rule (4). Given  $d' > 0$ , the strongest constraint comes from the largest value of  $z$ . We adopt the model-independent distance  $D_A(0, 1090) = 12.8 \pm 0.07$  Mpc from the cosmic microwave background (CMB) [25] and the locally measured Hubble parameter  $H_0 = 72.5 \pm 2.5$  km/s/Mpc [26]. (We give error bars as 68% limits and ranges as 95% limits.) These values do not depend on the assumption that the Universe at late times is well described by the FLRW metric on large scales. Taking the  $2\sigma$  lower bound for both quantities, we have  $d > 3.1$ , which implies  $k < 0.10$ . (In fact, the conservative bounds  $D_A > 12$  Mpc and  $H_0 > 60$  km/s/Mpc would be sufficient for  $k < 0.1$ .)

*Probability distribution for  $k$ :* The  $\chi^2$  for the SN data is the same for all three lens models, but for the lensing data, the  $\chi^2$  is 78, 20, and 11 for models Ia, Ib, and II, respectively. Given that we have 30 lensing data points, model Ia underestimates the statistical errors, there are systematic problems with the lensing data or the FLRW metric does not apply. In any case, the increased errors of model Ib and the greater complexity of model II seem to overcompensate. A look at outliers indicates that the issue is probably systematics. For model Ia, there are seven lenses that are outliers at more than  $2\sigma$ . If the reason was problems with the FLRW metric, we would expect the outliers to show a distinct pattern in redshifts. Instead, they are distributed randomly, as we would expect if the problem is unmodeled systematic issues with the lenses. A 2D Kolmogorov-Smirnov test indicates that, for model Ia, the probability that the outliers and nonoutliers are drawn from the same distribution is 29% [27]. In fact, the lenses' goodness of fit does not form a pattern for any of the lensing models. We, therefore, conclude that the data does not provide evidence for deviations from the FLRW metric. We produce a conservative truncated list of lenses by removing the most extreme outlier, refitting and iterating until all lenses are within  $2\sigma$ . This leaves us with 23 lenses for model Ia. For models Ib and II, we use all 30 lenses, as none are outliers.

We marginalize over the three polynomial coefficients to obtain the probability distribution  $P(k)$ . The results are shown in Fig. 1. Even without a prior on  $k$ , the probability distribution is not Gaussian, and has a tail at negative values of  $k$ . The 95% ranges, mean and best-fit values for  $k$ , as well as the goodness-of-fit values are given in Table I. Our studies of mock data sets show that, for current data, the typical offset of the mean and the best-fit from the real underlying values is much smaller than the error bars. Imposing the prior on  $k$  leads to an increase in  $\chi^2$  for model Ia, indicating tension between the lensing and CMB data. There is no such issue in model II, but given its large number of parameters, and possible systematic issues with the lenses, it would be premature to conclude that it is more realistic.

For model Ia, we have  $-0.63 < k < 1.22$ , or  $-0.97 < k < 0.08$  with the prior. For model Ib, the range increases

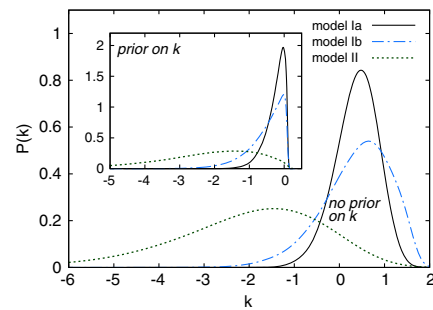


FIG. 1 (color online). Probability distribution of  $k$ , using the SIE model (black, solid line), SIE model with additional 20% error (blue, dotted-dashed line) and the model of [19] (green, dotted line). The inset shows the case with the prior  $k < 0.1$ .



TABLE I. Results for  $k$  for different lens models, with and without the prior from CMB and  $H_0$ . In  $\chi^2$ , the subscript SN refers to SNe,  $L$  refers to lenses and tot refers to both. The number of SN data points is 580. The number of lensing data points is 23 for model Ia and 30 for models Ib and II.

Model	Best fit	Mean	95% range	$\chi^2_{\text{SN}}$	$\chi^2_L$	$\chi^2_{\text{tot}}$	Prior on $k$
Ia	0.55	0.38	[−0.63, 1.22]	545	23	568	None
Ib	0.76	0.37	[−1.42, 1.54]	545	20	565	None
II	−1.34	−2.06	[−5.98, 0.61]	545	11	556	None
Ia	0.09	−0.25	[−0.97, 0.08]	545	28	573	$k < 0.1$
Ib	0.09	−0.53	[−1.92, 0.07]	545	21	566	$k < 0.1$
II	−1.34	−2.29	[−6.07, 0.13]	545	11	556	$k < 0.1$

by a factor of 1.6. For model II, there is a long negative tail, due to degeneracy between decreasing  $N$  and increasing  $-k > 0$ . There is no evidence for spatial curvature.

For comparison, if we assume that the Universe has FLRW geometry, that the Einstein equation holds, and that the matter consists of dust and vacuum energy, we obtain  $-0.53 < k < 0.52$  for models Ia and Ib and  $-0.55 < k < 0.51$  for model II. In this case, the constraints on  $k = -\Omega_{K0}$  are dominated by the SN data, the lensing data is unimportant.

*Conclusions.—Results and comparison to previous work:* The  $k_s$  test based on the distance sum rule (3) for the FLRW metric is independent of the matter content of the Universe and its relation to spacetime geometry on cosmological scales, though general relativity has been assumed to be valid when determining  $d_{ls}/d_s$  from astrophysical systems. We find that the data is consistent with the FLRW metric. Treating lenses as SIE with the published errors and eliminating outliers, the spatial curvature parameter  $\Omega_{K0} = -k$  is determined to be  $-1.22 < \Omega_{K0} < 0.63$  from SN and lensing data, and  $-0.08 < \Omega_{K0} < 0.97$  when we include a prior from CMB and  $H_0$ . These numbers are sensitive to lens modeling.

This range is 2 orders of magnitude wider than the one quoted from the latest CMB plus baryon acoustic oscillation data,  $-0.007 < \Omega_{K0} < 0.006$  [28]. That assumes that the Universe is described by a FLRW model whose late-time matter content is dust and vacuum energy, and that the Einstein equation is valid on cosmological scales. However, tight constraints,  $-0.007 < \Omega_{K0} < 0.01$ , are also obtained in an analysis with loose priors on dark energy, combining WMAP7 CMB, Union2 SN and big bang nucleosynthesis data as well as local  $H_0$  measurements [29]. Without the  $H_0$  value, which is debated [26,30,31], the constraint is  $-0.12 < \Omega_{K0} < 0.01$ . The sensitivity is due to two distinct effects. First, the overall angular scale of the CMB anisotropy pattern provides a measurement of the angular diameter distance to  $z = 1090$ , which depends strongly on the spatial curvature via the hyperbolic sine in (2) [32]. (Note that the labels for the two curvature parameters in Table I of [32] should be swapped.) However, if the Universe is not well described by a FLRW model, it is possible that spatial curvature evolves so that it is only

significant at late times, and is not strongly constrained by high-redshift probes [4]. Second, the large-angle anisotropy of the CMB is sensitive to spatial curvature via the late integrated Sachs-Wolfe (ISW) effect, which is particularly important in [29]. However, analysis of the ISW effect depends on assumptions about evolution of dark energy perturbations, which are rather speculative, particularly if the equation of state crosses  $-1$ .

Model-independent constraints based only on geometrical optics, such as the ones provided here or obtained from comparison of distance with expansion rate [6–8,31] or cosmic parallax [9], are, thus, complementary to model-specific analyses, which involve more assumptions about the matter content and the theory of gravity.

*Future constraints:* In addition to strong lensing image deformation by galaxies, existing observations of time delays, and both strong and weak lensing by galaxy, groups and clusters can be used to improve the constraints. Strong lensing by clusters may be promising, because individual lenses have several sources and some of the lenses are tightly modeled. On the other hand, many source redshifts are higher than current independent measurements of  $d_s$ . The Euclid satellite, set to launch in 2020, is expected to observe  $10^5$  strong lensing systems [33]. The usefulness of these systems for the test discussed here depends on follow-up observations to determine lens properties. Better understanding of the systematics of modeling lensing systems will be crucial. Given such progress, we can expect constraints on deviations from the FLRW metric, and on the spatial curvature of the FLRW universe, to significantly improve in the near future from the proof of concept we have presented here. Assuming lens model Ia and a spatially flat FLRW model with dust and vacuum energy,  $10^4$  SNe [34] and  $10^4$  lensing data points with current errors give the constraint  $-0.03 < \Omega_{K0} < 0.04$ , within a factor of a few of the current model-dependent range.

We thank Artem Kupri for help with selecting and analyzing the lensing systems, Josiah Schwab for providing the measured values of  $\delta$ , and Adam Bolton for correspondence. A.F. acknowledges support from the Finnish Academy, Grant No. 266918. K.B. thanks the Australian Research Council for support through the Future Fellowship (Grant No. FT140101270). Computational resources used in this work were provided by Intersect Australia Ltd.

- [1] F. Ferrer and S. Räsänen, Dark energy and decompactification in string gas cosmology, *J. High Energy Phys.* 02 (2006) 016; F. Ferrer, T. Multamäki, and S. Räsänen, Fitting oscillating string gas cosmology to supernova data, *J. High Energy Phys.* 04 (2009) 006; F. Ferrer, Cosmological acceleration from a gas of strings, *Nucl. Phys. B, Proc. Suppl.* 194, 218 (2009).
- [2] K. Enqvist, Lemaitre-Tolman-Bondi model and accelerating expansion, *Gen. Relativ. Gravit.* 40, 451 (2008); S. February,

- J. Larena, M. Smith, and C. Clarkson, Rendering dark energy void, *Mon. Not. R. Astron. Soc.* **405**, 2231 (2010); K. Bolejko, M.-N. C el erier, and A. Krasinski, Inhomogeneous cosmological models: Exact solutions and their applications, *Classical Quantum Gravity* **28**, 164002 (2011); M. Redlich, K. Bolejko, S. Meyer, G. F. Lewis, and M. Bartelmann, Probing spatial homogeneity with LTB models: A detailed discussion, *Astron. Astrophys.* **570**, A63 (2014).
- [3] S. R as anen, Light propagation in statistically homogeneous and isotropic dust universes, *J. Cosmol. Astropart. Phys.* **02** (2009) 011; Light propagation in statistically homogeneous and isotropic universes with general matter content, *J. Cosmol. Astropart. Phys.* **03** (2010) 018; T. Buchert and S. R as anen, Backreaction in late-time cosmology, *Annu. Rev. Nucl. Part. Sci.* **62**, 57q (2012); M. Lavinto, S. R as anen, and S. J. Szybka, Average expansion rate and light propagation in a cosmological Tardis spacetime, *J. Cosmol. Astropart. Phys.* **12** (2013) 051.
- [4] C. Boehm and S. R as anen, Violation of the FRW consistency condition as a signature of backreaction, *J. Cosmol. Astropart. Phys.* **09** (2013) 003.
- [5] C. Clarkson, B. A. Bassett, and T. C. Lu, A General Test of the Copernican Principle, *Phys. Rev. Lett.* **101**, 011301 (2008).
- [6] A. Shafieloo and C. Clarkson, Model independent tests of the standard cosmological model, *Phys. Rev. D* **81**, 083537 (2010).
- [7] E. M ortsell and J. J onsson, A model independent measure of the large scale curvature of the Universe, [arXiv:1102.4485](https://arxiv.org/abs/1102.4485).
- [8] D. Sapone, E. Majerotto, and S. Nesseris, Curvature vs distances: Testing the Copernican Principle, *Phys. Rev. D* **90**, 023012 (2014).
- [9] S. R as anen, A covariant treatment of cosmic parallax, *J. Cosmol. Astropart. Phys.* **03** (2014) 035.
- [10] P. J. E. Peebles, *Principles of Physical Cosmology* (Princeton University Press, Princeton, NJ, 1993).
- [11] G. Bernstein, Metric tests for curvature from weak lensing and baryon acoustic oscillations, *Astrophys. J.* **637**, 598 (2006).
- [12] N. Suzuki *et al.* (Supernova Cosmology Project), The Hubble space telescope cluster supernova survey: V. Improving the dark energy constraints above  $z > 1$  and building an early-type-hosted supernova sample, *Astrophys. J.* **746**, 85 (2012).
- [13] I. M. H. Etherington, On the definition of distance in general relativity, *Philos. Mag.* **15**, 761 (1933); reprinted in *Gen. Relativ. Gravit.* **39**, 1055 (2007); G. F. R. Ellis, *General Relativity and Cosmology*, edited by R. K. Sachs (Academic Press Inc., London, 1971), p. 104, reprinted in *Gen. Relativ. Gravit.* **41**, 581 (2009).
- [14] S. Nadathur and S. Sarkar, Reconciling the local void with the CMB, *Phys. Rev. D* **83**, 063506 (2011).
- [15] G. R. Bengochea, Supernova light-curve fitters and dark energy, *Phys. Lett. B* **696**, 5 (2011); Z. Li, P. Wu, and H. Yu, Probing the course of cosmic expansion with a combination of observational data, *J. Cosmol. Astropart. Phys.* **11** (2010) 031; M. C. March, R. Trotta, P. Berkes, G. D. Starkman, and P. M. Vaudrevange, Improved constraints on cosmological parameters from SNIa data, *Mon. Not. R. Astron. Soc.* **418**, 2308 (2011); R. Giostri, M. Vargas dos Santos, I. Waga, R. R. R. Reis, M. O. Calvao, and B. L. Lago, From cosmic deceleration to acceleration: New constraints from SN Ia and BAO/CMB, *J. Cosmol. Astropart. Phys.* **03** (2012) 027.
- [16] C. S. Kochanek, P. Schneider, and J. Wambsganss, 2004, *Part 2 of Gravitational Lensing: Strong, Weak & Micro, Proceedings of the 33rd Saas-Fee Advanced Course*, edited by G. Meylan, P. Jetzer, and P. North (Springer-Verlag, Berlin, 2004).
- [17] C. S. Kochanek, E. E. Falco, C. D. Impey, J. Lehar, B. A. McLeod, H.-W. Rix, C. R. Keeton, J. A. Munoz, and C. Y. Peng, The fundamental plane of gravitational lens galaxies and the evolution of early-type galaxies in low density environments, *Astrophys. J.* **543**, 131 (2000).
- [18] E. O. Ofek, H.-W. Rix, and D. Maoz, The redshift distribution of gravitational lenses revisited: Constraints on galaxy mass evolution, *Mon. Not. R. Astron. Soc.* **343**, 639 (2003).
- [19] J. Schwab, A. S. Bolton, and S. A. Rappaport, Galaxy-scale strong lensing tests of gravity and geometric cosmology: Constraints and systematic limitations, *Astrophys. J.* **708**, 750 (2010).
- [20] See Supplemental Material at <http://link.aps.org/supplemental/10.1103/PhysRevLett.115.101301> for the lensing data.
- [21] A. S. Bolton, S. Burles, L. V. E. Koopmans, T. Treu, R. Gavazzi, L. A. Moustakas, R. Wayth, and D. J. Schlegel, The Sloan lens ACS survey. V. The full ACS strong-lens sample, *Astrophys. J.* **682**, 964 (2008).
- [22] <http://simbad.u-strasbg.fr/simbad/sim-fid>.
- [23] J. Schwab (private communication).
- [24] C. Catto en and M. Visser, Cosmography: Extracting the Hubble series from the supernova data, [arXiv:gr-qc/0703122](https://arxiv.org/abs/gr-qc/0703122); S. Nesseris and J. Garc a-Bellido, Comparative analysis of model-independent methods for exploring the nature of dark energy, *Phys. Rev. D* **88**, 063521 (2013).
- [25] M. Vonlanthen, S. R as anen, and R. Durrer, Model-independent cosmological constraints from the CMB, *J. Cosmol. Astropart. Phys.* **08** (2010) 023; B. Audren, J. Lesgourgues, K. Benabed, and S. Prunet, Conservative constraints on early cosmology with MONTE PYTHON, *J. Cosmol. Astropart. Phys.* **02** (2013) 001; B. Audren, Separate constraints on early and late cosmology, *Mon. Not. R. Astron. Soc.* **444**, 827 (2014).
- [26] G. Efstathiou,  $H_0$  revisited, *Mon. Not. R. Astron. Soc.* **440**, 1138 (2014).
- [27] W. H. Press, S. A. Teukolsky, W. T. Vetterling, and B. P. Flannery, *Numerical Recipes: The Art of Scientific Computing*, 3rd ed. (Cambridge University Press, New York, 2007).
- [28] P. A. R. Ade *et al.* (Planck Collaboration), Planck 2013 results. XVI. Cosmological parameters, *Astron. Astrophys.* **571**, A16 (2014).
- [29] P. M. Okouma, Y. Fantaye, and B. A. Bassett, How flat is our Universe really?, *Phys. Lett. B* **719**, 1 (2013).
- [30] V. C. Busti, C. Clarkson, and M. Seikel, Evidence for a lower value for  $H_0$  from cosmic chronometers data?, *Mon. Not. R. Astron. Soc.* **441**, L11 (2014).
- [31] A. Heavens, R. Jimenez, and L. Verde, Standard Rulers, Candles, and Clocks from the Low-Redshift Universe, *Phys. Rev. Lett.* **113**, 241302 (2014).
- [32] C. Clarkson, T. Clifton, A. Coley, and R. Sung, Observational constraints on the averaged Universe, *Phys. Rev. D* **85**, 043506 (2012).
- [33] <http://sci.esa.int/euclid/>.
- [34] [http://lsst.org/lstt/science/scientist\\_supernovae/](http://lsst.org/lstt/science/scientist_supernovae/).